Engineering Structures 240 (2021) 112414

Contents lists available at ScienceDirect

Engineering Structures

journal homepage: www.elsevier.com/locate/engstruct

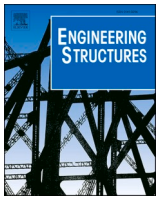

An accelerated corrosion-fatigue testing methodology for offshore wind applications

Ali Mehmanparast *, Azenor Vidament

Offshore Renewable Energy Engineering Centre, Cranfield University, Cranfield, Bedfordshire MK43 0AL, UK

ARTICLE INFO

Keywords:
Corrosion-fatigue
Acceleration testing
Temperature effects
Seawater
Offshore structures

ABSTRACT

Offshore wind turbines are subjected to cyclic loading conditions during their operational lifespan which is typically between 20 and 25 years. An important issue in fatigue design and integrity assessment of offshore wind turbine foundations is the examination of the long-term fatigue and corrosion-fatigue behaviour of steel structures in the high cycle region. High cycle fatigue tests, particularly at low frequencies in a seawater environment, are time-consuming and costly. Therefore, there is an essential need to perform accelerated tests to predict the long-term behaviour of the structures under realistic operational loading conditions. In this work, the existing fatigue acceleration mechanisms have been reviewed and a novel methodology has been proposed for accelerated testing and analysis of fatigue data in different environments (i.e. air, salt-spray and seawater) at higher temperatures. Two distinct equations have been developed and proposed for the calibration and prediction of S-N fatigue life and crack growth behaviour of steels in different environments. The proposed methodology has been validated through comparison with the existing data in the literature and predictions have been made at operational temperatures using high temperature data. The proposed approach is relatively simple to calibrate for a material of interest and enables accelerating S-N fatigue and crack growth testing of the examined materials by a factor of two and three, respectively. The proposed methodology and the obtained results have been discussed in terms of the need for accelerated testing for fatigue design and integrity assessment of offshore wind monopiles, especially those which are close to the end of initial design life and need a comprehensive engineering analysis for life extension or decommissioning.

1. Introduction

In 2019, the global offshore wind installed capacity reached a new record of 30,000 MW [1], which is about twice the installed capacity in 2016. Knowing that several projects for large offshore wind farms have been launched and new farms are under construction, such as the expansion of the Hornsea project in the UK, the exponential growth in offshore wind capacity is expected to continue in the coming years. The majority of the installed offshore wind turbines (i.e. over 80%) are supported by monopile foundations while the remaining minority are supported using other types of foundations including jackets [2]. The offshore wind farms are typically designed for 20 to 25 years of operation under extreme loading conditions due to the constant exertion of wind, wave and current loads which induce fatigue damage in the installed structures [3]. As the first generation of offshore wind farms which were installed in the late 1990s and early 2000s are quickly approaching their end of initial design life, questions are being raised regarding the realistic estimate of the remaining life of the installed offshore wind turbines by considering the over-conservative assumptions employed during the design process. This means that the offshore wind monopile foundations could presumably operate for a longer period, hence studies are being conducted on the possibility of life extension for existing wind farms rather than decommissioning the offshore wind infrastructure upon reaching the end of initial design life.

In this context, it is important to understand the behaviour of materials employed in fabrication of monopiles under fatigue loading conditions in air and seawater environments [4]. The fatigue tests must replicate the operational loading conditions, meaning the wind and wave spectra as well as the rotational intervals of the rotor must be considered in the test design. The SLIC (Structural Lifecycle Industry Collaboration) joint industry project was recently formed with the overall aim of achieving a better understanding of fatigue and fracture behaviour of offshore wind monopiles, particularly in air [5]. While performing fatigue tests in air are relatively simple, corrosion-fatigue

* Corresponding author.
E-mail address: a.mehmanparast@cranfield.ac.uk (A. Mehmanparast).

https://doi.org/10.1016/j.engstruct.2021.112414
Received 27 September 2020; Received in revised form 19 March 2021; Accepted 15 April 2021
Available online 30 April 2021

tests are often conducted in artificial sea water prepared in accordance with ASTM D1141 "Standard Practice for the Preparation of Substitute Ocean Water" recommendations [6]. Corrosion-fatigue tests for offshore wind applications are typically performed at 0.1–0.3 Hz to account for wave excitation frequency [7]. The low frequency range in corrosion-fatigue tests results in a low number of cycles per unit of time. This means that a longer period of time is required in order to achieve a certain number of cycles in corrosion-fatigue tests, hence these tests take much longer to complete compared to higher frequency tests in air.

It is known that for a given material, loading condition and surface finish (in the case of welded joints), the fatigue damage in air is dependent on the number of cycles. Therefore, an effective approach to shorten fatigue experiments in air is to increase the test frequency. Although cyclic testing at higher frequencies can effectively reduce the amount of time needed to conduct fatigue tests in air, this approach cannot be applied to corrosion-fatigue tests due to the low test frequencies required for such tests in seawater. In other words, corrosion-fatigue damage is dependent on the number of cycles (which drives the fatigue damage) as well as time (which drives the corrosion damage). Therefore, increasing the frequency in corrosion-fatigue tests would discard the contribution of corrosion damage to the overall failure, and consequently the results from corrosion-fatigue tests at high frequencies would be very similar to those results obtained from the fatigue tests in air.

While the increase in frequency cannot be used as an acceleration mechanism in corrosion-fatigue tests, the experimental data available in the literature indicate that an increase in seawater temperature, would reduce the fatigue life and increase the crack growth rate [8]. Therefore, the main aim of this study is to explore the influence of temperature on the fatigue performance of engineering material and subsequently develop an accelerated test method for performing corrosion-fatigue tests in much shorter time scales. In order to achieve this goal, the fatigue test data at different temperatures on various materials have been collated and analysed in this study and new models have been proposed to quantify the extent of acceleration in uniaxial S-N fatigue and fracture mechanics-based fatigue crack growth tests in seawater by changing the test temperature. The results have been discussed with a view to proposing a novel corrosion-fatigue acceleration mechanism by increasing the temperature in seawater corrosion-fatigue tests and suggest a practical approach to enhance the corrosion-fatigue life predictions for offshore wind turbine monopile foundations.

2. Corrosion and fatigue mechanisms

2.1. Corrosion of offshore materials

The material used in the fabrication of offshore wind monopile foundations is mainly S355 structural carbon steel [4]. Although corrosion protection mechanisms by means of surface coating and cathodic protection are considered in the design of offshore wind turbine foundations, which are the parts of the structure in direct contact with seawater, such corrosion protections normally break down after a certain duration of operation and subsequently corrosion damage occurs in the offshore wind turbine foundations before the corrosion protections are repaired. The corrosion mechanism is the result of an electrochemical reaction to a transfer of one or several electrons taking place in two stages; the anodic and cathodic half-reaction. During the process, electrons transit from the anode to the cathode [9]. Two half-equations (anodic and cathodic) which describe the chemical reactions during the corrosion process in steels employed in offshore wind turbine foundations are given below:

$$Fe \rightarrow Fe^{2+} + 2\,e^{-} \tag{1}$$

$$O_2 + 2\,H_2O + 4\,e^{-} \rightarrow 4\,OH^{-} \tag{2}$$

Thus, the resulting reactions from the combination of those two half-reactions, which leads to creation of the rusts, are:

$$2\,Fe + O_2 + 2\,H_2O \rightarrow 2\,Fe + 4\,OH^{-} = 2\,Fe(OH)_2 \tag{3}$$

$$4\,Fe(OH)_2 + 2\,H_2O + O_2 \rightarrow 4\,Fe(OH)_3 = 2\,Fe_2O_3(H_2O) + 4\,H_2O \tag{4}$$

Therefore, the resumed chemical reaction which occurs during the corrosion of steel is:

$$Fe + 3\,O_2 + 2\,H_2O = 2\,Fe_2O_3(H_2O) \tag{5}$$

As it can be seen above, the presence of oxygen within the seawater is necessary for the corrosion damage to happen. Nonetheless, in the case of a fully immersed steel-made structure, a corrosion mechanism will still occur in the absence of dissolved oxygen but at a slower rate. In fully immersed offshore wind turbine foundations, the cathodic reaction would be replaced by a hydrogen reduction by:

$$2H^{+} + 2\,e^{-} \rightarrow H_2 \tag{6}$$

Corrosion damage is known to be very sensitive to the temperature. The temperature dependency in the corrosion process is due to the fact that the dissolution of the metal (anodic reaction) is activated by increasing the temperature, whilst the reduction of oxygen (cathodic reaction) is slowed down. Therefore, increasing the temperature reduces the solubility of oxygen in water, and therefore prevents the cathodic reaction from taking place [10].

2.2. The principles of fatigue

Offshore structures are subjected to cyclic service loading conditions which would introduce a progressive failure mechanism known as fatigue. During the operational lifespan of offshore wind turbines, fatigue damage occurs in these structures which would lead to the initiation of cracks at the outer surface of the structures followed by crack growth and eventual failure. The fatigue damage mechanism can be divided into three mains stages: i) initiation of surface cracks which can be originated from micro defects introduced during the fabrication processes such as welding, ii) growth of the existing cracks, and iii) global failure.

The major time-consuming stage in fatigue life is the crack initiation stage and once the crack is initiated the growth process is relatively rapid compared to the overall lifetime of the structure. Therefore, the life expectancy of engineering components and structures, including offshore wind monopiles, is designed using S-N curves which are in fact empirical curves which correlate the applied stress range, S, with the number of cycles to failure, N. The relationship between the stress range and the number of cycles to failure can be described using a power-law equation:

$$S^{n}N = C_0 \tag{7}$$

where n and C_0 are the power-law constants which depend on the material, surface finish and the test environment. The S-N curve power-law constants for design purposes can be found in international standards such as the DNVGL RP-C203 [11] and BS 7608 [12].

The crack growth behaviour of materials subjected to fatigue loading conditions can be characterised by correlating the fatigue crack growth per cycle da/dN with the linear elastic fracture mechanics parameter ΔK, where a is the crack length, N is the cycle number and ΔK is the stress intensity factor range. A schematic illustration of the fatigue crack growth behaviour in engineering material is shown in Fig. 1. As seen in this figure, the fatigue crack starts to propagate when the stress intensity factor range is above the threshold value, ΔK_{th}, below which the crack growth would not take place. Subsequently, the crack propagates in a relatively steady manner which can be described using a power-law relationship between da/dN and ΔK which appears as a straight line in log–log axes. The fatigue crack growth in the secondary region, which is also known as the Paris region, continues until an exponential and unsteady crack growth starts to occur in the tertiary region which would

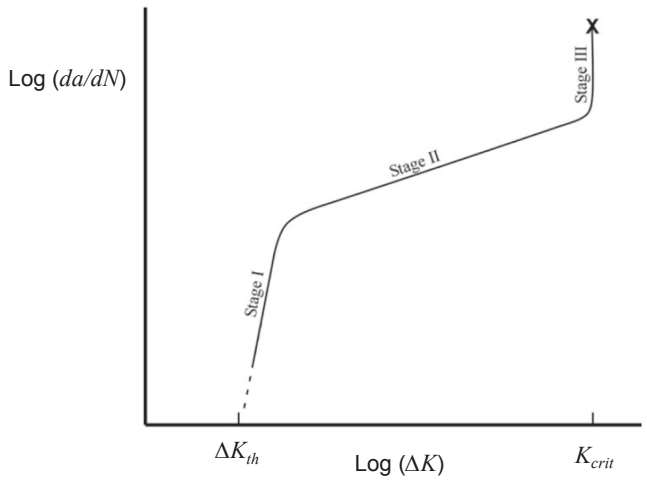

Fig. 1. Different stages of fatigue crack growth.

eventually lead to failure when the stress intensity factor reaches a critical value, K_{crit}.

The power-law relationship in the Paris region, which is often referred to as the Paris law, can be described as:

$$\frac{da}{dN} = A\Delta K^m \tag{8}$$

where A and m are material constants which are determined empirically. The Paris law constants for various materials, operational conditions and environments can be found in international standards such as BS 7910 [13].

2.3. Corrosion-fatigue interaction

Corrosion-fatigue is an interactive failure mechanism which occurs due to combined cycle-dependent fatigue damage and time-dependent corrosion damage. In fact, under corrosion-fatigue loading conditions the higher fatigue crack growth rate, compared to the air condition, results from the superposition of a local plastic deformation ahead of the crack tip and the electrochemical reaction due to corrosion damage. There are several models available in the literature which describe the corrosion-fatigue phenomenon in steels due to the anodic dissolution and the hydrogen embrittlement.

The anodic dissolution, which is also known as the film rupture model, is a mechanism during which the protected film created by corrosion at the crack-tip is cyclically fissured by the applied stresses from fatigue loads. Once the film is ruptured, the bare metal is in contact with the corrosive solution, leading to an increase in the crack length rate. This process repeatedly occurs during the corrosion-fatigue phenomenon [9]. As for the hydrogen embrittlement, it is described by the absorption of a hydrogen atom by the metal near the crack-tip zone, leading to fragilization and making the fracture easier for the fatigue mechanism. In the corrosion-fatigue phenomenon, both corrosion and fatigue damage mechanisms occur simultaneously; however, depending on the applied load level, test duration and applied frequency, one of the two models may play a more dominant role during the corrosion-fatigue process.

Corrosion-fatigue tests are less commonly performed, compared to fatigue tests in air, due to the fact that they are costly and time-consuming, though according to the recommendations available for S-N fatigue design curves in international standards such as DNVGL RP-C203 [11] and BS 7608 [12] a factor of three reduction in fatigue life, compared to the air environment, is applied for the free-corrosion environment. Having said that, there is insufficient experimental evidence in the literature to confirm how conservative this fatigue life reduction penalty is, particularly for the large number of cycles corresponding to 20–25 years of operation in offshore wind turbines.

2.4. Acceleration mechanisms for corrosion-fatigue testing

As mentioned earlier, fatigue tests in air can be accelerated simply by increasing the test frequency; however, the frequency in corrosion-fatigue tests must be kept at a relatively low value, hence such tests are rather time-consuming. Therefore, it is quite essential to find an alternative mechanism for shortening the duration of corrosion-fatigue experiments. It is known that corrosion-fatigue test duration is sensitive to electrochemical and physical factors such as electrolyte composition, pH, oxygen concentration, external polarization and temperature [14]. The influence of each of these factors on corrosion-fatigue has been briefly explained below with a view to identifying an effective approach for accelerating corrosion-fatigue tests.

2.4.1. Salt-spray method

One way of performing accelerated corrosion-fatigue tests is by exposing the sample to salt-spray prior to testing and then performing the fatigue test in air. This process is known as an “uncoupled” test method where corrosion and fatigue damage do not take place concurrently [15]. The salt-spray pre-corrosion test is relatively quick and low cost, but it does not represent the realistic environmental conditions where corrosion-fatigue takes place in an industrial application. On the other hand, salt-spray can also be used “coupled” with fatigue loads [16], but it requires a salt-spray chamber to be installed around the test specimen on the fatigue machine. The salt-spray test method is in fact an accelerated corrosion mechanism where the corrosive attack is enhanced compared to seawater and the crack initiation and growth accelerates due to the higher chloride ion concentration [17]. This method is particularly used for coated metals following the procedures outlined in ASTM B117 [18], as it enables establishing a rapid comparison between the corrosion resistance of the coating of interest and the uncoated metal.

2.4.2. Applied potential method

The applied potential method is occasionally used to control and monitor a corrosion-fatigue experiment, but it has been proven to influence the corrosion-fatigue behaviour of the material [19]. The application of a small current through the specimen during a corrosion-fatigue test will influence the test duration and it might increase or decrease the crack growth rate depending on the material and test conditions. Using this test method, the polarisation of the specimen is achieved by a montage between a potentiostat, the specimen (i.e. the working electrode), a reference electrode (to measure the potential) and a sacrificial electrode.

Guo *et al.* carried out corrosion-fatigue tests on HRB400 high strength steel, at the frequency of 10 Hz, in different environments including air, distilled water, 3.5% NaCl and accelerated corrosive environment using the applied potential method [20]. The accelerated test set-up in their experiments consisted of the specimen (anode) which was immersed in 3.5% NaCl solution, a stainless-steel plate (cathode) and a direct current of 0.5 A between the two, while cyclic loads were applied on the test specimen. The results showed that by increasing the aggressiveness of the environment, the fatigue crack growth rate was also increased, especially near the threshold region. The aggressiveness of the environment also has an influence on the threshold value itself and it was reported that ΔK_{th} was decreased when the applied potential acceleration mechanism was implemented in the experiments [20].

2.4.3. Oxygen concentration

Oxygen is a major component in the corrosion reaction of steels through the anodic dissolution mechanism, therefore the oxygen concentration influences the corrosion rate in metals. As the dissolved oxygen concentration is reduced, the crack growth rate also decreases in

the absence of oxygen at the crack tip [21]. At room temperature, the normal oxygen concentration is about 7–8 ppm. Although a small change in the oxygen content of the electrolyte does not affect the crack growth rate, a large reduction in oxygen dissolved concentration down to a concentration of 3–1 ppm would drastically alter the corrosion-fatigue crack growth rate.

2.4.4. Temperature

Although the influence of temperature on the corrosion-fatigue behaviour of materials has been investigated in a number of previous studies, none of the existing works available in the literature were aimed at using temperature as an acceleration mechanism for corrosion fatigue testing. Vosikosky *et al.* [22] investigated the effect of seawater temperature on corrosion-fatigue crack growth for BS4360 : 50D structural steel. Their tests were performed in artificial seawater (3.5% NaCl), at 0 °C and 25 °C with 0.1 Hz frequency. Their results showed that while at both temperatures the crack growth rate was about four times higher in a seawater environment compared to air, the increase in temperature increased the crack growth rate by a factor of around two both in air and seawater [22].

2.5. Research motivation for the present study

Conducting corrosion-fatigue experiments at a low frequency is costly and time-consuming particularly for developing S-N curves where multiple tests at various stress levels are required, unlike crack growth tests where the monitored data from a single test can be analysed while the test is running. Therefore, finding an effective way to accelerate corrosion-fatigue experiments especially to study S-N curves in seawater would be extremely beneficial and could be used to optimise the design of future generations of offshore wind monopiles by reducing the level of excess conservatism in the design process. Following the review of the existing corrosion-fatigue acceleration mechanisms given above, the focus of this study is to quantitatively analyse and predict the extent of corrosion-fatigue acceleration by means of increased temperature, which has shown a great potential to shorten the test duration but has not yet been employed in any studies as an acceleration mechanism. Therefore, the existing corrosion-fatigue S-N and crack growth data for a range of steels tested at various temperatures are collated and presented below with a view to designing future experiments by increasing the seawater temperature as an acceleration mechanism.

3. Materials and methodology

Three main datasets were selected from previous studies regarding fatigue life (i.e. S-N curves) in order to develop a robust methodology to quantitatively analyse the temperature effects on the fatigue behaviour of steel in different environments such as air, seawater and salt-spray. The selection of three independent datasets was to examine the reliability of the proposed methodology to predict the fatigue acceleration due to temperature effects on a range of steels. For each selected database, the proposed methodology has been applied to calibrate the model and derive the corresponding material model constants for a given test environment. Similar to S-N fatigue analysis, two datasets from previous studies were selected to investigate the dependency of fatigue crack growth on the test temperature in air and seawater environments. The proposed methodology for examination of the temperature effects on S-N fatigue life and fatigue crack growth is explained below.

3.1. S-N fatigue life

3.1.1. Selected materials

The first S-N fatigue dataset was taken from the experimental study conducted by Micone *et al.* [15] on high-strength low-alloy (HSLA) steel type DNV F460. These tests were performed in natural seawater from the North Sea at a frequency of $f = 10$ Hz with the stress ratio of $R = 0.1$ in the temperature range of 15–45 °C. Before performing the fatigue experiments, the specimens were immersed in seawater until a corrosion layer was formed on the outer surface of the test specimens. The second dataset was taken from the work conducted by Wu *et al.* [16] who carried out experiments on FV520B steel in seawater and salt-spray environments. These tests were performed using sinusoidal waveforms with a frequency of $f = 110$ Hz in the temperature range of 25–150 °C. From these experiments Wu *et al.* concluded that the temperature effect on S-N fatigue data was noticeable both in seawater and salt-spray environments. Wu *et al.* developed a life prediction model for the salt-spray environment, taking into consideration the influence of the temperature, which is described as [16]:

$$N_f = \left(1-\left(\frac{\sigma_a}{\sigma_c(T)}\right)^{f(T)}\right)\left(\frac{2\pi nF\rho f}{3M}\left(\pi\left(\frac{\Delta K_{th}}{4.4K_t\sigma_a}\right)^2\right)^3\left(\frac{1}{I_p}\right) + \frac{a_c^{(1-m_1/2)}}{c_1\Delta\sigma^{m_1}\beta_1^{m_1}K_t^{m_1}\pi^{m_1/2}(m_1/2-1)}\right) + \left(\frac{\sigma_a}{\sigma_c(T)}\right)^{f(T)}\left(\frac{\sigma_a}{2268}\right)^{-1/0.12451} \quad (9)$$

where N_f is the total number of cycles to failure, σ_a is the stress amplitude (in MPa), M is the atomic mass of the material, n is the number of electrons released during the corrosion process, F is the Faraday constant, ρ is the density of the metal, f is the frequency (in Hz), ΔK_{th} is the stress intensity factor range threshold value, K_t is the stress concentration factor, I_p is the pitting current, a_c is the corrosion weight factor, $\Delta\sigma$ is the stress range, β_1 is the crack geometry factor and m_1, c_1 are material constants. In Eq. (9), $\sigma_c(T)$ is the critical stress related to the temperature and $f(T)$ is the temperature coefficient which can be calculated by:

$$f(T) = 40.2977 - 0.1633T + 1.9509x10^{-4}T^2 \quad (10)$$

$$\sigma_c(T) = -2525.4405 + 15.376T - 0.0184T^2 \quad (11)$$

where T is the temperature. Although this model showed a good correlation with the experimental data in a salt-spray environment, the proposed model by Wu *et al.* is complex and difficult to calibrate for different materials and environments, hence there is need for a simpler model to describe the fatigue life dependency of steels on temperature.

The third dataset employed in this study was taken from the work conducted by Ghaleeh [23]. These experiments were performed on Sn-37Pb alloy in air at a frequency range of 1–2 Hz with a stress ratio of $R = 0.15$ in the temperature range of 25–75 °C. From these experiments it was observed that the fatigue life decreases exponentially by increasing the test temperature.

3.1.2. Proposed methodology

The correlation between the stress range, S, and the number of cycles to failure, N, can be described by the Basquin equation shown in Eq. (7) where n and C_0 are material constants. Although the material constants in the Basquin equation, which are the basis of S-N design curves for engineering structures, are available in different international standards such as [11,12], the existing values in such standards are not material-specific (i.e. they have been provided for a wide range of materials) and the variations in exact temperatures at which the tests were conducted to derive S-N curves are unknown. This means that especially for design purposes, the proposed S-N design curves in international standards might be overly conservative as they account for the worst case scenario in the fatigue data which could have been obtained in a particular material or due to temperature fluctuation. In other words, knowing that the temperature influences the S-N fatigue data, the results obtained at so-called "room temperature" might differ depending on the season (e.g. summer vs. winter) and the country where the tests were conducted. Therefore, there is an essential need to consider the temperature effects on S-N fatigue behaviour of a given material of interest.

In this work, a simplified approach has been proposed to account for the temperature effects on the S-N fatigue behaviour of engineering

materials using a modified form of Basquin equation, which can be described as:

$$T^p S^n N = C_T \tag{12}$$

where T is the temperature in °C, and p and C_T are temperature-dependent constants. It is worth noting that for simplicity, the proposed model in this work suggests assuming that the stress exponent n is a fixed value which can be calculated as the mean value of average stress exponents obtained from different temperatures. The material and temperature-dependent constants in Eq. (12) can be obtained by applying linear regression fits to the experimental data points.

3.2. Crack growth rate curves

3.2.1. Selected materials

The first fatigue crack growth dataset was taken from the work presented by Appleton on BS4360 : 50D steel in seawater [21]. These tests were performed in 3% NaCl seawater under free corrosion condition at the frequency of $f = 0.167$ Hz with the stress ratio of $R = 0.5$ in the temperature range of 7–60 °C. Appleton's work showed that the secondary fatigue crack growth region, which is also known as the Paris region, was strongly dependent on the temperature and accelerated crack growth rates were observed at higher temperatures. The second dataset was taken from the work conducted by Zeng *et al.* on AZ61 Magnesium alloy in air [24]. These tests were conducted at the frequency of $f = 1$ Hz with the stress ratio of $R = 0$ and maximum applied load level of $P_{max} = 7$ kN in the temperature range of 25–120 °C. The results also showed that the crack growth behaviour of the material is sensitive to the test temperature.

3.2.2. Proposed methodology

Atkinson and Lindley [25] suggested a model to describe the influence of temperature on the corrosion-fatigue crack growth behaviour of the material by assuming that the total corrosion-fatigue crack growth rate, $\left(\frac{da}{dN}\right)_{CF}$ is the summation of the crack growth rate proportion due to cyclic loads (which is also known as Paris law) and crack growth rate proportion due to environmental condition (i.e. seawater). Their proposed model was described as:

$$\left(\frac{da}{dN}\right)_{CF} = A\Delta K^m + \frac{f}{2}\frac{da}{dt} \tag{13}$$

where ΔK is the stress intensity factor range, f is the frequency, and A and m are material-dependent Paris law constants and $\frac{da}{dt}$ is described as:

$$\frac{da}{dt} = B exp\left(-\frac{Q}{RT}\right) \tag{14}$$

where Q is the apparent enthalpy activation in J/mole, R is the universal molar gas constant in J/mol.K, T is the temperature in Kelvin and B is a constant.

It can be seen in Eq. (13) that the fatigue crack growth rate in a corrosive environment is frequency-dependent. However, it is evident from experimental data that by increasing the frequency in a corrosive environment, the crack growth rate will be closer to the test data in air, which is in contradiction with Eq. (13). Moreover, although the model proposed by Atkinson and Lindley takes into consideration the fatigue crack growth dependency on temperature, it does not accurately describe the time-dependency (i.e. frequency effects) in corrosive environments.

Jakubowski developed an empirical model [26], mostly based on the work of Thomas and Wei [27], which described the combined effect of the frequency f and the temperature T on the fatigue crack growth rate in a corrosive environment. Based on Jakubowski's model, the fatigue crack growth rate in the secondary region can be described as:

$$\frac{da}{dN} = \left(\frac{da}{dN}\right)_{Air}\left(\frac{0.1}{f}\right)^k\left(\frac{\Delta K}{\Delta K_{II-III}}\right)^{-n} exp\left(\frac{E(T-T_R)}{RTT_R}\right) \tag{15}$$

where $\left(\frac{da}{dN}\right)_{Air}$ is the fatigue crack growth rate in air, n, k and ΔK_{II-III} are constants, E is the activation energy in kJ/mole, T_R and T are the room temperature and test temperature, respectively, and R is the universal molar gas constant.

Another method of explaining the temperature dependency in the fatigue crack growth behaviour of materials was proposed by Fertig [28] where a potential connection between the kinetic theory of fracture and Paris Law was employed to predict the crack growth dependency on the test frequency, R-ratio and temperature. In his model, the Paris Law exponent was kept as a contact value regardless of the environmental conditions.

In the present study, two experimental datasets available in the literature were collated and analysed to propose a simplified temperature-dependent model which describes the fatigue crack growth behaviour of steels in the Paris region as:

$$\frac{da}{dN} = A_T \Delta K^m T^y \tag{16}$$

where T is the temperature in °C, and y and A_T are temperature-dependent constants. It must be noted that for simplicity, the model proposed in this work suggests assuming that the stress intensity factor range exponent m is a fixed value which can be calculated as the mean value of average stress intensity factor range exponents obtained from different temperatures.

4. Temperature effects on fatigue life and crack growth behaviour

4.1. S-N curves

4.1.1. Air environment

The experimental dataset taken from the work conducted by Ghaleeh on Sn-37Pb in the air [23] was analysed and the effect of temperature on the fatigue life was examined using the proposed model shown in Eq. (12). These tests were performed at 25 °C (i.e room temperature), 35 °C and 75 °C. A line of best fit was initially made to the data points and Basquin constants n and C_0 (see Eq. (7)) were identified for each temperature and are summarised in Table 1. As explained earlier, the proposed model in this study assumes that the stress exponent is independent of the variation in temperature for simplicity. Therefore, new lines of best fit were made to the data points using the average value of individual stress exponents at different temperatures and the power-law constants obtained using the fixed-slope stress exponent, denoted *n-fixed and* $C_{0,\ n\text{-}fixed}$, are presented in Table 1. Upon completion of the first step of the analysis, the number of cycles to failure N was correlated with temperature T for different values of stress ranges (i.e. taking stress range as a constant) and the temperature-dependent power-law constants in Eq. (12), p and C_T, were identified and are shown in Table 2.

Following identification of the material and temperature-dependent power-law constants, the fatigue life prediction for Sn-37Pb alloy in air obtained from the temperature-dependent model proposed in this work (see Eq. (12)) can be described as:

Table 1
Basquin power-law constants for fatigue tests in air using Eq. (7).

Temperature (°C)	n	Log(C_0)	*n-fixed*	Log($C_{0,\ n\text{-}fixed}$)
25	12.17	17.52	12	17.34
35	14.20	19.47	12	17.08
75	10.28	14.38	12	16.25

Table 2
Temperature-dependent power-law constants for fatigue tests in air using Eq. (12).

p	C_T
2.31	4.0×10^{20}

$$N = 4.0 \times 10^{20} \frac{1}{S^{12}} \frac{1}{T^{2.31}} \quad (17)$$

The experimental data from fatigue tests in air at different temperatures are compared with the calibrated temperature-dependent prediction model (see Eq. (17)) and the results are shown in Fig. 2. The coefficients of determination, R^2, for the fatigue life prediction lines obtained from Eq. (17) are 0.983, 0.951 and 0.993 for 25 °C, 35 °C and 75 °C, respectively, indicating that the proposed model accurately describes the fatigue life of the examined material in air at different temperatures.

It can be seen in Fig. 2 that the influence of temperature on the fatigue life of a given material tested in air is quite significant and an increase in the test temperature will shift the S-N curve to the left resulting in a substantial reduction in fatigue life for a given value of stress range. Fig. 2 shows that the fatigue life of the examined material in air has reduced by around an order of magnitude by increasing the test temperature from 25 °C to 75 °C. This means that a slight change in the test temperature will have a significant effect on the fatigue life expectancy of the material. Moreover, it must be noted that the temperature dependency in fatigue life varies from one material to another and the constants in the proposed model shown in Eq. (12) needs to be calibrated for the material of interest.

4.1.2. Salt-spray environment

The experimental dataset taken from the work performed by Wu *et al.* [16] on FV520B steel in a salt-spray environment was analysed and the effect of temperature on the fatigue life was examined using the proposed model shown in Eq. (12). These tests were performed at 25 °C, 75 °C and 150 °C. Linear regression analysis was initially performed on the fatigue data and the Basquin constants n and C_0 (see Eq. (7)) were identified for each temperature. Following this, the power-law constants were re-evaluated by fixing the stress exponent. The Basquin constants from the regression analysis, before (n and C_0) and after fixing the stress exponent (n-*fixed* and $C_{0,\ n\text{-}fixed}$), are summarised in Table 3. Subsequently, by taking the stress range as a constant value, the number of cycles to failure N was correlated with the temperature T and the temperature-dependent power-law constants in Eq. (12), p and C_T, were identified and are shown in Table 4.

Using the identified material and temperature-dependent power-law constants, the fatigue life prediction for FV520B steel in a salt-spray environment can be described as:

Table 3
Basquin power-law constants for fatigue tests in a salt-spray environment using Eq. (7).

Temperature (°C)	n	Log(C_0)	n-*fixed*	Log($C_{0,\ n\text{-}fixed}$)
25	4.05	17.33	4	17.19
75	4.30	17.76	4	16.93
150	3.95	16.37	4	16.50

Table 4
Temperature-dependent power-law constants for fatigue tests in salt-spray environment using Eq. (12).

p	C_T
0.84	2.5×10^{18}

$$N = 2.5 \times 10^{18} \frac{1}{S^{4}} \frac{1}{T^{0.84}} \quad (18)$$

The comparison of the experimental data from fatigue tests in a salt-spray environment with the temperature-dependent fatigue life prediction model are shown in Fig. 3. The coefficients of determination, R^2, for the fatigue life prediction lines obtained from Eq. (18) are 0.873, 0.974 and 0.959 for 25 °C, 75 °C and 150 °C, respectively. These R^2 values of close to unity indicate that the fatigue life of the examined material in a salt-spray environment can be accurately described using the proposed model which has been shown in the general form in Eq. (12).

It can be seen in Eq. (18) and Fig. 3 that for the salt-spray environment, an increase in the test temperature results in a substantial reduction in fatigue life for a given value of stress range. Fig. 3 shows that for the examined material in a salt-spray environment, by increasing the test temperature from 25 °C to 75 °C and 150 °C the fatigue life reduces by a factor of around two and five, respectively. This shows that similar to S-N fatigue tests in air, the fatigue life in a salt-spray environment is very sensitive to the test temperature and the reduction in the number of cycles to failure can be accurately predicted using the proposed model shown in Eq. (12).

4.1.3. Seawater environment

The experimental data taken from Micone *et al.* [15] on DNV F460 steel tested in seawater were analysed to investigate the effect of temperature on corrosion-fatigue life of steels. These tests were performed at 15 °C and 45 °C. A line of best fit was firstly made to the data available at each temperature and the Basquin constants n and C_0 were quantified for each temperature and subsequently re-evaluated by fixing the slope of the S-N curves using the average value of individual stress exponents obtained from the initial analysis. The Basquin constants from the initial regression analysis (n and C_0) and after fixing the stress exponent (n-

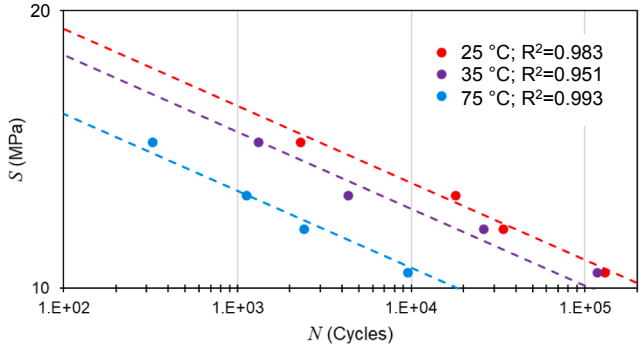

Fig. 2. Comparison of the fatigue data in air on Sn-37Pb alloy with the temperature-dependent fatigue life prediction model at 25 °C, 35 °C and 75 °C.

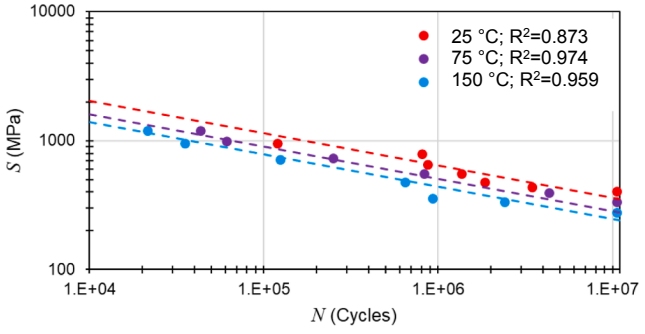

Fig. 3. Comparison of the fatigue data in salt-spray environment on FV520B steel with the temperature-dependent fatigue life prediction model at 25 °C, 75 °C and 150 °C.

Table 5
Basquin power-law constants for fatigue tests in seawater environment using Eq. (7).

Temperature (°C)	n	Log(C_0)	n-fixed	Log($C_{0,\ n\text{-}fixed}$)
15	4.66	17.94	5	18.84
45	5.92	21.14	5	18.72

fixed and $C_{0,\ n\text{-}fixed}$), are summarised in Table 5. Subsequently, similar to the procedure described in Section 4.1.1 the number of cycles to failure N was correlated with the temperature T and the temperature-dependent power-law constants in Eq. (12), p and C_T, were identified and are shown in Table 6.

Using the identified material and temperature-dependent power-law constants, the fatigue life prediction for DNV F460 steel in a seawater environment can be described as:

$$N = 1.4 \times 10^{19} \frac{1}{S^5} \frac{1}{T^{0.26}} \tag{19}$$

The comparison of the experimental data from fatigue tests in a seawater environment with the prediction lines are shown in Fig. 4. The coefficients of determination, R^2, obtained for the prediction lines using Eq. (19) are 0.987 and 0.951 for 15 °C and at 45 °C, respectively, implying that the model developed for the seawater environment, which is shown in the general form in Eq. (12), presents an excellent correlation with the experimental data. It can be clearly seen in Eq. (19) and Fig. 4 that the temperature has a considerable influence on the fatigue life of DNV F460 steel in seawater and the number of cycles to failure decrease by increasing the temperature of the seawater. Furthermore, the results in Fig. 4 show that for a given stress range, an increase in the seawater temperature from 15 °C to 45 °C results in a reduction in fatigue life by around 25%.

4.2. Fatigue crack growth

4.2.1. Air environment

The fatigue crack growth experimental data taken from the work conducted by Zeng *et al.* on AZ61 Magnesium alloy in air [24] was analysed to investigate the temperature effect on the fatigue crack growth behaviour of the material. These tests were performed at 25 °C, 60 °C and 120 °C. Following the procedure explained in Section 3.2.2, the Paris law constants m and A were initially obtained using regression analysis on the data points available at different temperatures. Following this, the power-law constants were re-evaluated by taking the average of stress intensity factor range exponents from different temperatures as the fixed exponent in the analysis. The power-law constants from the secondary fatigue crack growth data before (m and A) and after fixing the power-law exponent (m-*fixed* and $A_{m\text{-}fixed}$) are summarised in Table 7. Subsequently, the fatigue crack growth rate da/dN was correlated with temperature T and the temperature-dependent power-law constants in Eq. (16), y and A_T, were identified and are shown in Table 8.

Using the material and temperature-dependent power-law constants summarised in Table 7 and Table 8, the fatigue crack growth rate for AZ61 Magnesium alloy in air can be described as:

$$\frac{da}{dN} = 2.9 \times 10^{-6} \Delta K^{1.2} T^{0.46} \tag{20}$$

The plot of the prediction model and the experimental fatigue crack growth data in air can be seen in Fig. 5. It can be seen in this figure that the fatigue crack growth prediction lines are in good agreement with the experimental data. Moreover, it can be observed in this figure that the fatigue crack growth behaviour of the material is very sensitive to the temperature and greater crack growth rates are observed at higher temperatures. Fig. 5 and Eq. (20) show that increasing the test temperature from 25 °C to 120 °C results in an increase in the fatigue crack growth rate by a factor of around two. The observed results indicate that a variation in temperature during fatigue crack growth tests may have a noticeable impact on the obtained test results.

Table 6
Temperature-dependent power-law constants for fatigue tests in a seawater environment using Eq. (12).

p	C_T
0.26	1.4×10^{19}

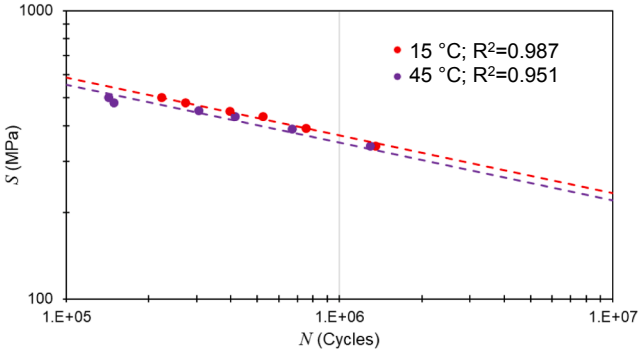

Fig. 4. Comparison of the fatigue data in seawater environment on DNV F460 steel with the temperature-dependent fatigue life prediction model at 15 °C and 45 °C.

Table 7
Paris law constants for fatigue crack growth tests in air.

Temperature (°C)	m	Log(A)	m-fixed	Log($A_{m\text{-}fixed}$)
25	1.13	−4.765	1.2	−4.836
60	1.15	−4.782	1.2	−4.824
120	1.26	−4.611	1.2	−4.505

Table 8
Temperature-dependent power-law constants for fatigue crack growth tests in air using Eq. (16).

y	A_T
0.46	2.9×10^{-6}

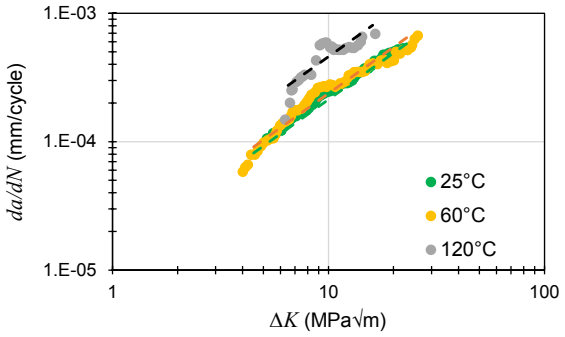

Fig. 5. Comparison of the fatigue crack growth data in air on AZ61 Magnesium alloy with the temperature-dependent prediction model at 25 °C, 60 °C and 120 °C.

4.2.2. Seawater environment

The corrosion-fatigue crack growth data on BS4360:50D steel in seawater taken from [21] were analysed to explore the influence of

temperature on the corrosion-fatigue crack growth behaviour of the material. These tests were performed at 7 °C, 23 °C, 40 °C and 60 °C. Similar to the analysis on the air data, the Paris Law constants were initially worked out using the line of best fit made to the data and subsequently regression analysis was conducted by assuming a constant power-law exponent obtained from the average value of stress intensity factor range exponents at different temperatures. The secondary region fatigue crack growth power-law constants before (m and A) and after fixing the exponent (m-*fixed* and $A_{m\text{-}fixed}$) are summarised in Table 9. Following completion of the first step of the analysis, the fatigue crack growth rate da/dN was correlated with the temperature T and the temperature-dependent power-law constants (y and A_T in Eq. (16)) were identified and are shown in Table 10.

Using the power-law constants summarised in Table 9 and Table 10, the fatigue crack growth rate for AZ61 Magnesium alloy in seawater can be described as:

$$\frac{da}{dN} = 1.1 \times 10^{-8} \Delta K^{2.5} T^{0.53} \tag{21}$$

The corrosion-fatigue crack growth rates predicted from the model are compared with the experimental data points at various temperatures in Fig. 6. As seen in Eq. (21) and Fig. 6, the corrosion-fatigue crack growth rate in seawater is very sensitive to the change in the temperature and for the examined material da/dN increases by a factor of around three as a result of an increase in temperature from 7 °C to 60 °C. Also seen in Fig. 6 is that while the test data at 7 °C have appeared to be much lower than the rest of the data at higher temperatures, the fatigue crack growth rates at 23 °C, 40 °C and 60 °C have fallen close to each other, particularly in the lower stress intensity factor range region. Having said that, it is evident from the experimental data that the fatigue crack growth rate in seawater continuously increases with an increase in temperature.

5. Discussion

It is evident from the results shown in Section 4 that the proposed methodology provides an accurate prediction of fatigue life in steel structures at different temperatures in air and corrosive environments. Knowing that the proposed model presented in Eq. (12) for S-N fatigue life and (16) for fatigue crack growth are material and temperature-dependent, it is essential to calibrate the model using the experimental data obtained from the material of interest. It is worth noting that based on the results presented in this study, although the fatigue behaviour in all of the examined materials has been found to be sensitive to the temperature, this effect has been found to be more pronounced in some of the materials and test environments compared to others. Therefore, for the material of interest preliminary tests must be conducted to examine the extent of change in fatigue life in different environments (i.e. air, salt-spray and seawater).

There are a number of advantages to using this proposed technique for the fatigue life assessment of engineering structures. The first advantage of the proposed methodology is that it is fairly simple and easy to follow by other researchers and practitioners. The second advantage is that the models presented in Eqs. (12) and (16) take into account the temperature dependency of fatigue life and crack growth behaviour in different environments, and are not limited to only one environment. The third advantage is that relatively limited experimental data on at least two temperatures would be sufficient to quantify the temperature-dependent constants in Eqs. (12) and (16). Of course by feeding more experimental data in a wider range of temperatures the level of accuracy will be improved and less error will be observed between the prediction lines and the actual data points. Last but yet importantly, the most practical application of the proposed methodology is to predict the S-N fatigue life and crack growth behaviour of steel structures at the operational temperature by performing accelerated tests at higher temperatures. While there are alternative ways for accelerating fatigue tests in air, for instance by increasing the test frequency, the approach proposed in this study delivers significant beneficial impact for corrosion-fatigue testing which must be conducted at low frequencies to allow time-dependent corrosion damage to interact with cycle-dependent fatigue damage. Accelerated corrosion-fatigue testing will be cost-effective and saves the time needed to characterise the fatigue life of structures at lower temperatures.

In order to highlight the significance of the proposed accelerated fatigue testing approach, the S-N corrosion-fatigue prediction lines for the material examined in Section 4.1.3 are presented for a wide range of temperatures in Fig. 7. In this figure, the predicted S-N curves at 15 °C and 45 °C for which the experimental data were available (see Fig. 4) are shown in dashed lines whereas the predicted S-N curves at other temperatures are presented in dotted lines. As seen in this figure, for a given value of stress range the fatigue life of the material continuously reduces

Table 9
Paris law constants for fatigue crack growth tests in seawater.

Temperature (°C)	m	$Log(A)$	m-*fixed*	$Log(A_{m\text{-}fixed})$
7	1.99	−6.875	2.5	−7.549
23	1.92	−6.465	2.5	−7.213
40	2.84	−7.538	2.5	−7.061
60	4.21	−9.437	2.5	−7.093

Table 10
Temperature-dependent power-law constants for fatigue crack growth tests in seawater using Eq. (16).

y	A_T
0.53	1.1×10^{-8}

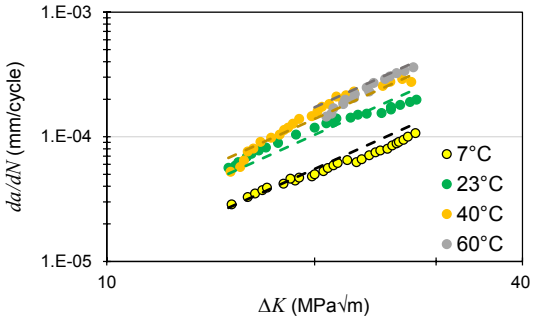

Fig. 6. Comparison of the corrosion-fatigue crack growth data in seawater on BS4360 50D steel with the temperature-dependent prediction model at 7 °C, 23 °C, 40 °C, 60 °C.

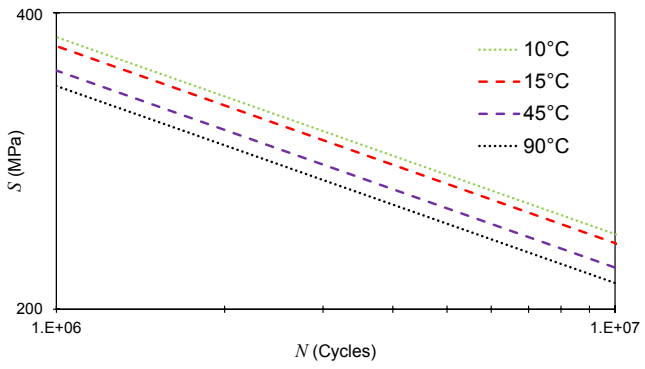

Fig. 7. Prediction of fatigue life in seawater environment for DNV F460 steel in a wide range of temperatures.

by increasing the seawater temperature. The S-N curves presented in Fig. 7 indicate that the fatigue life of offshore structures made of this type of steel in a seawater environment with an operational temperature of 10 °C (which is typical of North Sea conditions [5,29]) can be predicted around twice faster by performing accelerated tests at 90 °C (which is sufficiently high, yet below the boiling temperature of seawater). It is worth noting that the seawater tests in the work by Micone *et al.* [15] were performed at the relatively high frequency of $f = 10$ Hz, therefore it is expected that the acceleration factor from the tests performed at higher temperatures would have been much greater if the tests were performed at low frequencies. The time saving benefit from accelerated tests is particularly important for performing S-N fatigue tests in the high cycle region, $N > 10^6$ cycles, where an individual test takes much longer to complete compared to high stress tests and yet a number of tests are required to derive the S-N curve for design and integrity assessment purposes. Similar to the S-N fatigue acceleration in seawater, the tests in air and salt-spray environments can also be accelerated by increasing the test temperature using the proposed methodology presented in this work.

As seen in Section 4.1 and Fig. 7, the S-N fatigue data available in the literature at different temperature in seawater environment are obtained from relatively short-term tests with the number of cycles to failure of close to or less than 10^6. Given that offshore wind turbine steel structures are designed for operational lifespans of between 20 and 25 years, there is an essential need to obtain more data points for a larger number of cycles (i.e. beyond 10^6 cycles) for design and life assessment purposes. According to the recommendations in international standards such as DNVGL RP-C203 [11] and BS 7608 [12], under free-corrosion condition the fatigue life of a steel structure is reduced by a factor of three, compared to the high stress S-N curve in the air condition, and this trend is extrapolated to low stress regions. While a factor of three life reduction may be considered as an overconservative assumption suggested by international standards, the proposed methodology in this study can be employed in the examination of realistic life reduction factors in the presence of free-corrosion condition, compared to air, and investigate whether the life reduction penalty in the high and low stress regions of the S-N curve would be above or below three when the structure is subjected to free-corrosion condition.

Similar to any other accelerated testing methodologies, a number of weaknesses might be associated with the proposed approach presented in this study. According to international standards such as DNVGL RP-C203 [11] and BS 7608 [12] the fatigue design life of steel structures operating in air and also seawater with cathodic protection can be described using bi-linear S-N curves in log–log axes, where a reduced slope is recommended for the high cycle (i.e. low stress) region. Although the proposed methodology is expected to provide accelerated test results with relatively high accuracy in the low cycle (i.e. high stress) region, where a greater slope is expected in the S-N curve, this approach may not be able to provide a reduced slope in the high cycle (i.e. low stress) region in air and in seawater under cathodic protection. Moreover, as explained in DNVGL RP-C203 [11] the slope in the high cycle region of the S-N curve in air and seawater under cathodic protection environments, heavily depends on the fatigue loading condition. Therefore, there is a likelihood that using the proposed accelerated testing approach, the high cycle region of the S-N curve in air and seawater under cathodic protection environments may exhibit a different slope compared to that observed in offshore wind turbine structures which are subjected to variable amplitude fatigue cycles during their lifespan. In order to examine the level of inaccuracies that might be induced using the proposed accelerated fatigue testing methodology in the high cycle region of the S-N curves in air, further tests will be conducted in future work at various temperatures and on different grades of steel and the results will be compared with real-life fatigue data obtained from actual steel structures.

Another interesting note is knowing that salt-spray itself is an approach for accelerating fatigue tests in a corrosive environment (which also allows performing high frequency tests for further acceleration of the tests), the increase in temperature in such tests is an additional mechanism that helps to complete fatigue tests in a corrosive environment within the quickest possible time frame. Therefore, further tests need to be conducted in future work to predict the seawater S-N curves from salt-spray tests which can be further accelerated by increasing the temperature and frequency.

The results presented in this study show that the increase in temperature does not only accelerate the S-N fatigue tests but also increases the fatigue crack growth rate in fracture mechanics tests. Although fatigue crack growth tests generally take a much shorter time to complete compared to low stress S-N fatigue tests, the proposed acceleration method proposed in this work facilitates the investigation of near threshold fatigue crack growth behaviour in a seawater environment which needs to be examined at low frequencies. The results presented in Fig. 6 indicate that for the examined type of steel, the fatigue crack growth rate da/dN at a given stress intensity factor range ΔK would increase by a factor of around three as a result of increasing the seawater temperature from 7 °C to 60 °C. This means that the fatigue crack growth behaviour of the material can be characterised in much shorter time scales by simply increasing the temperature to obtain accelerated data and predicting the actual crack growth behaviour of the engineering structure at lower operational temperatures from the model proposed in this study.

The proposed accelerated testing methodology presented in this study has been validated using the existing datasets on various types of steel available in a range of temperatures. The analysis does not include wind turbine steels due to the fact that such datasets are limited to a single temperature and have not been obtained from tests at various temperatures in previous studies [2,4,7,30–32]. Since the developed method in this study for fatigue life prediction by means of accelerated testing is quite novel, additional experiments must be performed on wind turbine steels in future work to confirm the fatigue and corrosion-fatigue trends in specialised materials used in offshore wind turbines. In order to apply this methodology to fatigue life prediction in offshore wind monopiles, further experiments must be conducted on structural steels which are widely used in the fabrication of these offshore structures in an artificial seawater environment, at low frequencies and at different selected temperatures. Monopiles are nowadays mainly made of different subgrades of S355 steel (see [30–35]). Therefore, it is recommended to perform S-N fatigue and crack growth tests in a range of temperatures in air and seawater primarily on S355 steel and alternatively on other wind turbine steels to build a more relevant material database for fatigue design and life assessment of offshore wind monopiles.

6. Conclusions

Fatigue tests are essential for the accurate design and integrity assessment of offshore structures. These tests can be time-consuming and costly, especially when performed at low frequencies in seawater. In order to accelerate the performance of fatigue tests, a novel methodology has been proposed in this work to obtain fatigue test results in much shorter time scales by performing tests at higher temperatures. Two models have been proposed for S-N fatigue life and crack growth prediction in steel structures by considering the influence of temperature on the test results. The proposed models have been validated through comparison with the existing experimental data in the literature at various temperatures. The results show that while an increase in temperature accelerates both S-N and fatigue crack growth in air, salt-spray and seawater environments, the fatigue behaviour of steel structures at operational temperatures can be predicted using the proposed methodology by performing a selected number of tests at higher temperatures. The proposed methodology is particularly valuable for the performance of low frequency corrosion-fatigue tests in seawater which are time-consuming. The results show that for the materials examined in

this study, the S-N fatigue and crack growth tests in seawater for typical operational temperature of around 10 °C can be predicted at least two and three times faster, respectively, by performing tests at higher temperatures. The proposed methodology suggests a practical approach for characterising the long-term behaviour of offshore structures, particularly offshore wind monopiles, at relatively low stress levels by performing tests in reasonable time frames and predicting the actual behaviour of the structure at lower operational temperatures.

CRediT authorship contribution statement

Ali Mehmanparast: Conceptualization, Methodology, Validation, Supervision, Writing - original draft, Writing - review & editing. **Azenor Vidament:** Formal analysis, Validation, Writing - review & editing.

Declaration of Competing Interest

The authors declare that they have no known competing financial interests or personal relationships that could have appeared to influence the work reported in this paper.

Acknowledgments

This work was supported by grant EP/L016303/1 for Cranfield, Oxford and Strathclyde Universities, Centre for Doctoral Training in Renewable Energy Marine Structures - REMS (http://www.rems-cdt.ac.uk/) from the UK Engineering and Physical Sciences Research Council (EPSRC).

References

[1] "Installed offshore capacity." [Online]. Available: https://www.irena.org/wind. (accessed on 26/09/2020).
[2] V. Igwemezie, A. Mehmanparast, and A. Kolios, "Current trend in o ff shore wind energy sector and material requirements for fatigue resistance improvement in large wind turbine support structures – A review," Renew. Sustain. Energy Rev., vol. 101, no. November 2018, pp. 181–196, 2019.
[3] L. Ziegler, E. Gonzalez, T. Rubert, U. Smolka, and J. J. Melero, "Lifetime extension of onshore wind turbines: A review covering Germany, Spain, Denmark, and the UK," Renew. Sustain. Energy Rev., vol. 82, no. January 2017, pp. 1261–1271, 2018.
[4] V. Igwemezie, A. Mehmanparast, and A. Kolios, "Materials selection for XL wind turbine support structures: A corrosion-fatigue perspective," Mar. Struct., vol. 61, no. June 2018, pp. 381–397, 2018.
[5] Mehmanparast A, Taylor J, Brennan F, Tavares I. "Experimental Investigation of Mechanical and Fracture Properties of Offshore Wind Monopile Weldments. SLIC Inter-Laboratory Test Results" 2018;41(12):2485–501.
[6] American Society For Testing and Materials - ASTM D1141, "Standard Practice for the Preparation of Substitute Ocean Water," ASTM Int., vol. 98, no. Reapproved 2013, pp. 1–3, 2013.
[7] V. Igwemezie and A. Mehmanparast, "Waveform and frequency effects on corrosion-fatigue crack growth behaviour in modern marine steels," Int. J. Fatigue, vol. 134, no. January, p. 105484, 2020.
[8] Thorpe TW, Scott PM, Rance A, Silvester D. Corrosion fatigue of BS 4360:50D structural steel in seawater. Int J Fatigue 1983;5(3):123–33.
[9] Anderson TL. Fracture mechanics: fundamentals and applications. Third 2017.
[10] O. T. Tsyrul'nyk, "Influence of Temperature on the Corrosion, Corrosion Fatigue, and Cavitation Fracture of Steel in tap water," Mater. Sci., vol. 36, no. 1, pp. 113–114, 2000.
[11] Det Norske Veritas (DNV)., "DNV-RP-C203: Fatigue design of offshore steel structures. Recommended practice," 2016.
[12] British Standards Institution (BSI), "BS 7608:2014+A1:2015 Standards Publication Guide to fatigue design and assessment of steel products," 2015.
[13] British Standards Institution (BSI), "BS-7190: Guide to methods for assessing the acceptability of flaws in metallic structures," BSI Stand. Publ., vol. 3, no. 1, p. 306, 2013.
[14] O. N. Romaniv, A. V Vol'demarov, and G. N. Nikiforchin, "Factors in Acceleration of Crack Growth during Corrosion Fatigue of High-Strength steels," Soviet materials science: a transl. of Fiziko-khimicheskaya mekhanika materialov/ Academy of Sciences of the Ukrainian SSR 16, no. 5, pp. 406-410, 1981.
[15] Micone N, De Waele W. Evaluation of Methodologies to Accelerate Corrosion Assisted Fatigue Experiments. Exp Mech 2016;57(4):547–57.
[16] Wu Q, Chen X, Fan Z, Nie D, Wei R. Corrosion fatigue behavior of FV520B steel in water and salt-spray environments. Eng Fail Anal 2017;79(March):422–30.
[17] Cui Y, Qin Y, Dilimulati D, Wang Y. The Effect of Chlorine Ion on Metal Corrosion Behavior under the Scratch Defect of Coating. Int. J. Corrosion 2019;2019.
[18] "Standard Practice for Operating Salt-spray (Fog) Apparatus 1," Annu. B. ASTM Stand., pp. 1–12, 2011.
[19] S. A. Shipilov, "Mechanisms for corrosion fatigue crack growth," Fatigue Fract. Eng. Mater. Struct., no. July 2001, pp. 243–259, 2002.
[20] Guo Z, Ma Y, Wang L, Zhang J, Harik IE. Corrosion Fatigue Crack Growth Mechanism of High-Strength Steel Bar in Various Environments Corrosion fatigue crack growth mechanism of high-strength steel bar in various environments. J Mater Civ Eng 2020;32.
[21] Appleton RJ. Corrosion fatigue of a C-Mn steel. University of Glasgow; 1985.
[22] Vosikovsky O, Neill WR, Carlyle DA, Rivard A. The Effect of Sea Water Temperature on Corrosion Fatigue-Crack Growth in Structural Steels. Can Metall Q 1987;26:251–7.
[23] Ghaleeh M. The durability of solder joints under thermo-mechanical loading; application to Sn-37Pb and Sn-3.8Ag-0.7Cu lead-free replacement alloy. Heriot-Watt University; 2015.
[24] Zeng R, Han E, Ke W. Effect of Temperature and Relative Humidity on Fatigue Crack Growth Effect of Temperature and Relative Humidity on Fatigue Crack Growth Behavior of AZ61 Magnesium Alloy. Mater Sci Forum 2007;546:409–12.
[25] Atkinson JD, Lindley TC. Effect of stress waveform and hold-time on environmentally assisted fatigue crack growth in C-Mn structural steel. Met. Sci. 1979;13(7):444–8.
[26] Jakubowski M. Corrosion fatigue crack growth rate characteristics for weldable ship and offshore steels with regard to the influence of loading frequency and saltwater temperature. Polish Maritime Res. 2017;24(93):88–99.
[27] Thomas JP, Wei RP. Corrosion fatigue crack growth of steels in aqueous solutions I: Experimental results and modeling the effects of frequency and temperature. Mater Sci Eng 1992;159:205–21.
[28] Fertig RS. Relating Paris Law Fatigue Crack Growth in Composites with a Physics-Based Fatigue Model. Proceedings of the American Society for Composites—Thirty-second Technical Conference. 2017.
[29] Mehmanparast A, Brennan F, Tavares I. Fatigue crack growth rates for offshore wind monopile weldments in air and seawater: SLIC inter-laboratory test results. Mater Des 2017;114:494–504.
[30] Jacob A, Oliveira J, Mehmanparast A, Hosseinzadeh F, Kelleher J, Berto F. Residual stress measurements in offshore wind monopile weldments using neutron diffraction technique and contour method. Theor Appl Fract Mech 2018;96:418–27.
[31] Igwemezie V, Dirisu P, Mehmanparast A. Critical assessment of the fatigue crack growth rate sensitivity to material microstructure in ferrite-pearlite steels in air and marine environment. Mater Sci Eng A 2019;754:750–65.
[32] Jacob A, Mehmanparast A, Urzo RD, Kelleher J. Experimental and numerical investigation of residual stress effects on fatigue crack growth behaviour of S355 steel weldments. Int J Fatigue 2019;128:105196.
[33] Jacob A, Mehmanparast A. Crack growth direction effects on corrosion-fatigue behaviour of offshore wind turbine steel weldments. Mar. struct. 2021;75:102881.
[34] Igwemezie V, Mehmanparast A, Brennan F. The role of microstructure in the corrosion-fatigue crack growth behaviour in structural steels. Mater. Sci. Eng.: A 2021;803:140470.
[35] Igwemezie V, Mehmanparast A, Brennan F. The influence of microstructure on the fatigue crack growth rate in marine steels in the Paris Region. Fatigue Fract. Eng. Mater. Struct. 2020;43:2416–40.